J Porous Mater (2016) 23:83–93
DOI 10.1007/s10934-015-0058-y

Functionalized mesoporous organo-silica nanosorbents for removal of chromium (III) ions from tanneries wastewater

Charles Gervas[1,2] · Egid B. Mubofu[1] · James E. G. Mdoe[1] · Neerish Revaprasadu[2]

Published online: 1 September 2015

Abstract Organo-silica mesoporous materials with cyano functional groups were prepared by a one pot co-condensation of 2-cyanoethyltriethoxysilane (CETS) and tetraethoxysilane (TEOS) at ratios of 1:4 and 1:9 using either sunflower oil or *n*-dodecylamine as templating agents. The tethered cyano groups were used as adsorption sites or hydrolysed to carboxylic surface functional groups. The prepared materials were characterized by diffuse reflectance infrared Fourier transform spectroscopy, atomic force microscopy (AFM), Brunauer, Emmettt and Teller, thermogravimetric analysis, transmission electron microscopy (TEM) and scanning electron microscopy (SEM). Results indicated that materials with cyano and carboxylic surface groups were successfully prepared. AFM results indicated that primary particles with irregular shapes and grain size ranging from 0.28 ± 0.03 to 0.46 ± 0.08 μm were obtained depending on the CETS to TEOS ratio used and the structure directing template. SEM and TEM micrographs depict spherical like morphology of the same size as portrayed by AFM results. Sunflower cyano functionalized micelle template silica (MTS-S-CN) at a ratio of 1:9 had surface area of 760.5 m^2/g and average pore diameters of 3.5 nm while MTS-S-CN at a ratio 1:4 had pore diameter of 10.1 nm with surface area of 734.1 m^2/g. On the other hand, the MTS-S-COOH (1:9) had surface area of 975.9 m^2/g with pore diameter of 4.6 nm whereas MTS-S-COOH (1:4) had surface area of 740.1 m^2/g with pore diameter of 6.3 nm. The materials were used in adsorption studies of Cr(III) ions from tannery wastewater. Cr(III) ions removal ranged from 48 to 83 % depending on the adsorbent functional group and the organosilyl groups to silica ratio. This study has indicated that materials prepared were good adsorbents with an adsorption maximum of 19.7 mg Cr(III) ions per g of adsorbent.

Keywords Mesoporous organo-silica · Nanosorbents · Tetraethoxysilane · Dodecylamine · 2-(Cyano ethyl triethoxysilane) · Tannery waste water · Chromium (III) ions

1 Introduction

Heavy metals are significant pollutants threatening the health of living organisms and affecting the environment in general. The growing awareness on the toxicity of heavy metals has led to increased interest in pollution abatement. Tannery effluents are the highest pollutants among all industrial wastes [1] and they are the large contributors of chromium ions pollution to the environment. Globally, the trend of the concentration of chromium metal ions escaping into the environment from tannery industries ranges between 2000 mg/L and 5000 mg/L which is far much higher than the recommended permissible discharge limits of 2 mg/L [1]. Trivalent chromium is one of the pollutants introduced into natural waters by a variety of industrial wastewaters like textile, leather tanning, electroplating and metal finishing industries [2–4].

Electronic supplementary material The online version of this article (doi:10.1007/s10934-015-0058-y) contains supplementary material, which is available to authorized users.

✉ Egid B. Mubofu
ebmubofu@gmail.com

[1] Chemistry Department, University of Dar es Salaam, P.O. Box 35061, Dar es Salaam, Tanzania

[2] Chemistry Department, University of Zululand, Private Bag X1001, Kwadlangezwa 3886, South Africa

Though tanning systems are of two types (vegetable tanning and chrome tanning), more than 90 % of global leather production is still carried out through chrome tanning process [4, 5]. Unfortunately, during this process of tanning only 60 % of the applied chrome salt is used and the remainder is sent to a depuration plant where the salts end up in the sludge [6]. This poses a major environmental problem in the tanning industry since the disposal of chromium contaminated sludge produced as a by product of waste water must be controlled, otherwise its disposal mechanism can be more hazardous to the environment especially water sources in the neighbourhood [7–10]. Recent detection of significant levels of toxic Cr(VI) in surface water and groundwater in different parts of the world has raised critical questions relating to the current disposal of Cr-containing wastes [6–9]. It has been established that despite the thermodynamic stability of Cr(III) species, the presence of certain naturally occurring minerals, especially manganese oxides, can enhance oxidation of Cr(III) to Cr(VI) in the soil. This is of public concern because at high pH, Cr(VI) is bioavailable, and it is this form that is highly mobile and therefore poses the greatest risk of groundwater contamination [9–12].

Many methods available for removal of heavy metals from aqueous media are expensive, non-selective, and are sometimes affected by the presence of other contaminants. Mesoporous nanoparticles prepared using organic surfactants are a new route in addressing the problem [13]. The route of preparation follows the discovery of MCM41 type of materials by the mobil company, by then using ionic surfactants [14–18]. Currently, non-ionic organic surfactants have proved effective towards the preparation of this important class of nanoparticles with multifaceted application including adsorption [15–20]. In order to get micelle templated silicas (MTS) with good properties, the surfactant should have a carbon chain length of not more than 18 (C_{18}) and not less than 8 (C_8). Generally, amorphous MTS and/or MTS with macropores are formed if the surfactant's carbon chain is short.

We hereby report the suitability of sunflower oil as a template for the preparation of organo-modified MTS. The capacity for adsorption of chromium (III) ions from Tanneries aqueous effluents of the materials was also established. The effects of contact time, amount of adsorbents and initial concentration of the chromium (III) ions are reported.

2 Experimental details

2.1 Materials, reagents and chemicals

All chemicals were of analytical grade and were used as received without further purification. Tetraethyl orthosilicate (TEOS) 98 %, *n*-dodecylamine, 2-(cyano ethyl triethoxysilane), sodium hydroxide, hydrochloric acid, absolute ethyl alcohol, sulfuric acid and *n*-hexane were purchased from Aldrich. Sunflower oil was extracted from sunflower seeds obtained from Dodoma region in Tanzania. Effluent of tanneries wastewater solution was collected from Kibaha Tanneries Industry, Coast Region in Tanzania.

2.2 Solvent extraction of sunflower oil

The extraction process involved washing the sunflower seeds with distilled water followed by grinding to increase the surface area for better solvent extraction of sunflower oil. The sunflower oil was extracted by the Soxhlet method using *n*-hexane as extracting solvent.

2.3 Synthesis of cyano-functionalized mesoporous silica (MTS-CN)

The synthesis of cyano-functionalized mesoporous silica was done via a one-pot co-condensation technique using sunflower oil as a templating agent as reported by other workers [16] with some modifications. In a typical experiment, a solution of sunflower oil (2.5 g) in aqueous ethanol (46 mL of absolute ethanol and 53 mL of distilled water) was stirred for about 45 min. Then, separately but simultaneously, TEOS (18.8 g, 0.09 mol) and 2-cyanoethyltriethoxysilane (CETS) (2.2 g, 0.01 mol) were added also rapidly along with a 0.01 g of sodium fluoride catalyst. The solution was maintained at a temperature of 45 °C at initial pH 10.2. The solution was stirred for 18 h and the white thick precipitate formed was vacuum filtered. The filtrate was then washed several times with large amount of ethanol. The template in the filtrates was removed by Soxhlet extraction for 9 h using ethanol as a solvent to get a fine white powder, hereinafter, MTS-S-CN (1:9). The powder was dried in an oven at 90 °C for 12 h before storing in a desiccator ready for characterization and post functionalization to carboxylic group. Using the same procedure, MTS-S-CN (1:4) was prepared at a 1:4 (CETS to TEOS) ratio.

Preparation of cyano functionalized mesoporous silica using *n*-dodecylamine (a commercial surfactant) as a template was also done for comparison purposes. The synthesis was done according to procedures described elsewhere [16] and no catalyst was employed. A heavy white cloudy precipitate was formed after 20 min; the work up procedure was done as described before. Schematic representation for the preparation of all cyano functionalized nanosorbent materials [MTS-S-CN (1:4), MTS-S-CN (1:9), MTS-DDA-CN (1:4) and MTS-DDA-CN (1:9)] is depicted in Fig. 1.

2.4 Conversion of the attached cyano functional group to carboxylic group

Hydrolysis of the cyano group to carboxylic group was performed by refluxing the material in 43 % (v/v) aqueous H_2SO_4 for 3 h. The mixture was cooled to room temperature, filtered and the modified material was dried over night at 90 °C and the dried solids were then stored in a desiccator prior to characterization and adsorption studies. Figure 2 shows the reaction conditions for attaching cyano and carboxylic group.

Hydrolysis of cyano functionalized nanosorbent materials prepared in Sect. 2.3 resulted into carboxylic functionalized materials namely MTS-S-COOH (1:4), MTS-S-COOH (1:9), MTS-DDA-COOH (1:4) and MTS-DDA-COOH (1:9).

2.5 Dilution of effluent from Kibaha tannery industry

The effluent of wastewater containing chromium ions collected from Kibaha Tannery industry was filtered using Whatman filter paper No. 1. Concentration of chromium was analyzed using Atomic Absorption Spectrophotometry (AAS) (Perkin Elmer, 2004). Analytical assurance was evaluated by using standard reference material from National Institute of Standard and Technology, USA. Samples were frozen waiting for analysis.

2.6 Characterization of organo-silica materials

Before analysis, the samples were dried overnight in a vacuum oven at 100 °C. The samples were then prepared by diluting the sample to about 10 % in KBr followed by grinding with pestle and motor to ensure thorough mixing. The diffusion reflectance infrared fourier transform spectroscopy (DRIFTS) was used to identify the –CN and –COOH functional groups present in the samples. For this purpose, a Perkin-Elmer 2000 FTIR spectrometer was used to collect data at the mid-IR region (3600–550 cm^{-1}) at resolution of 2 cm^{-1}/step with 16 scans. The DRIFT spectra of the MTS-S-CN and MTS-S-COOH samples were obtained by subtracting KBr background spectrum from the samples.

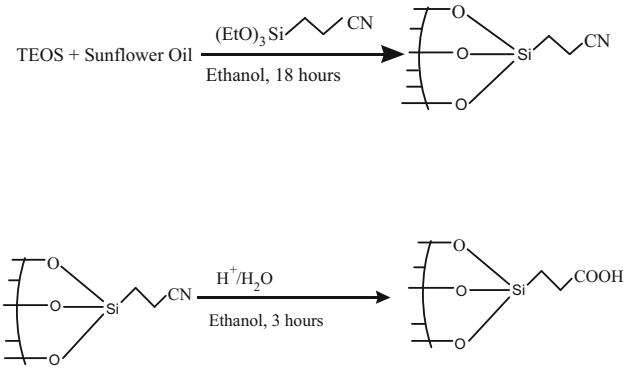

Fig. 2 Reaction scheme for the synthesis of MTS-S-CN and MTS-S-COOH

The grain size and morphology of the synthesized materials were determined by atomic force microscopy (AFM), using tapping mode. An AFM Version 3.0 Digital Instrument, Veeco Metrology Group was employed. A powdered sample of the material was fixed on a glass surface (about 1 cm^3) by using a transparent paper glue adhesive. Then the glass, on which the sample was fixed, was placed on the substrate holder of the AFM. The tapping tip was set and then engaged while the laser beam was

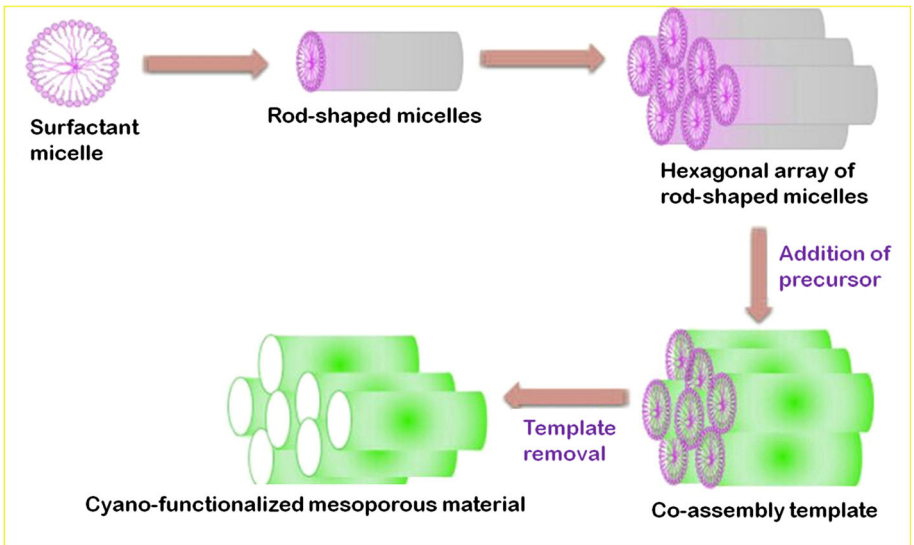

Fig. 1 Schematic representation of the process for the preparation of mesoporous materials

on. Software was employed to observe the real time images and offline version for further analysis. Brunnuer, Emmell and Teller (BET) and a Zeiss Ultra Plus FEG SEM were used to further discern the morphological structures of the materials. Thermogravimetric analyser (TGA) was also used to study the thermal stability of the prepared materials. The analyses were done using Perkin Elmer TGA Pyris 6 under nitrogen gas flow (20.0 mL/min) from 30.0 to 900.0 °C at a heating rate of 10 °C/min.

2.7 Adsorption experiments

Batch adsorption experiments were carried out by using a rotary shaker (FRAMCO SHAKER Baird & Tatlock (London) Ltd) set at 1500 rpm for approximately fixed time interval. Following a systematic process, the removal of chromium(III) ions from the tannery wastewater by using MTS-S-CN and MTS-S-COOH in a batch system was determined. The effects of different parameters (contact time, adsorbent dose and initial concentration) were also investigated. All experiments were conducted at room temperature.

2.7.1 Effect of contact time

Batch adsorption experiments were carried out at different contact times (from 2 to 180 min) for an initial concentration of Cr(III) ion in tannery wastewater ranging from 16 to 17.1 mg/L at pH 5.2. In a typical experiment, an appropriate amount of the adsorbent was mixed with 50 mL of the effluent of known concentration, in 100 mL round-bottom flask. The resulting mixture was then agitated at 1500 rpm and filtered using Whatman filter paper No. 50. The filtrate was analyzed by AAS to establish the amount of chromium(III) ions removed by the adsorbent.

2.7.2 Effect of amount of adsorbent

Batch adsorption experiments were done at different amounts of adsorbent ranging from 0.1 to 0.5 g in 50 mL tannery effluent solution containing 17.05 mg/L of chromium(III) ion solution at pH 5.2 the contact time was fixed at 30 min at room temperature. The samples were agitated at 1500 rpm, filtered and analyzed by AAS.

2.7.3 Effect of initial chromium(III) ion concentration

Batch experiments were conducted by contacting 0.1 g of adsorbent with 50 mL tannery wastewater solution containing chromium(III) ion at different initial concentrations (17.06, 28.42, 35.6, 44.2 and 52.8 mg/L) at pH 5.2 for a contact time of 30 min. The samples were agitated at 1500 rpm, filtered and analyzed by AAS.

2.8 Adsorption isotherm models

The Langmuir and Freundlich isotherm equations are common models used to find out the relationship between equilibrium concentrations of the adsorbate in liquid phase and in the solid phase. The Langmuir isotherm is valid for monolayer adsorption onto surface containing finite number of identical sorption sites and is presented by (Eq. 1).

$$q_e = \frac{q_m K_L C_e}{1 + K_L C_e} \tag{1}$$

where q_e is the amount of metal adsorbed per specific amount of adsorbent (mg/g), C_e is equilibrium concentration of the solution (mg/L), and q_m is the maximum of metal ions required to form a monolayer (mg/g). Equation (1) above can be linearised, thus determining the Langmuir constants (K_L) and the maximum monolayer adsorption capacity of adsorbent (q_m). These values can be determined by a linear plot of $1/q_e$ versus $1/C_e$. The values of q_m and K_L can be determined by a linear plot of $1/q_e$ versus $1/C_e$ (Eq. 2).

$$q_e = \frac{1}{q_m} + \frac{1}{q_m K_L C_e} = \frac{q_m K_L C_e}{1 + K_L C_e} \tag{2}$$

The Freundlich equation is purely empirical based on sorption on heterogeneous surface, which is commonly described by (Eq. 3).

$$q_e = K_f C_e^{1/n} \tag{3}$$

where, K_f and 1/n are the Freundlich constants related to adsorption capacity and adsorption intensity respectively. Linearizing Eq. (3) in logarithmic form is important to enable us determine the Freundlich constants, so it becomes (Eq. 4).

$$\text{Log}\, q_e = \text{Log}\, K_f + \frac{1}{n} \log C_e \tag{4}$$

The essential characteristics of the Langmuir isotherm parameters are normally used to predict the affinity between the sorbate and sorbent by using a dimensionless equilibrium parameter, 'RL' as given by the following equation:

$$R_L = \frac{1}{1 + K_L C_0} \tag{5}$$

where the value of R_L indicates the type of Langmuir isotherm to be irreversible ($R_L = 0$), favourable ($0 < R_L < 1$), linear ($R = 1$) or unfavourable ($R_l = 0$)

3 Results and discussion

3.1 Porosity properties of as prepared nanosorbents

The porosity properties of all prepared nanosorbents were determined by using BET method, whereby nitrogen

adsorption isotherms were used. Table 1 gives a summarized report of the BET surface area, pore volumes and average pore diameters of these materials.

Nanosorbents with higher surface area resulted in higher adsorptive of chromium (III) ions as compared to materials with low surface area. This difference in surface areas can be explained by the large concentration of TEOS which has an effect on the pore sizes and diameter of the nanoporous material. The shapes of the isotherms in Fig. 3 are in agreement with isotherms for the nanoporous materials. Figure 3 indicates the BET isotherms for MTS-S-CN (1:4), MTS-S-CN (1:9), MTS-S-COOH (1:4) and MTS-S-COOH (1:9).

The isotherms are identical, in that they rise rapidly when approaching $P/P_o = 1$. The shapes of the isotherms with hysteresis loops depict type IV isotherm loops which are typical for mesopores or MCM materials. Basically, the closure of the loop at $P/P_o \sim 0.4$ indicates the presence of small mesopores and the results presented in Table 1 depicts this phenomenon. The average pore diameter for the prepared nanosorbents ranged between 3.5 and 10.1 nm. The volume of nitrogen adsorbed depends on the pore diameter, pore volumes and surface area of the material. The isotherm loops look very similar in shape and sometimes they overlap, this is due to the fact that they are of the same material, the only difference is the concentration of TEOS, and functional groups (post functionalization of the materials). This indicates that the functional groups did not change the porosity nature of the material, though the ratio of TEOS and the functional groups had an effect on the surface area and hence their different rate of adsorption. Ratio of TEOS has negligible influence on the isotherm loops; however, it plays a crucial role on the pore size diameter and surface area. All nanosorbents prepared in this study had similar nitrogen adsorption–desorption hysteresis loops (ESI Fig. S1 & S2).

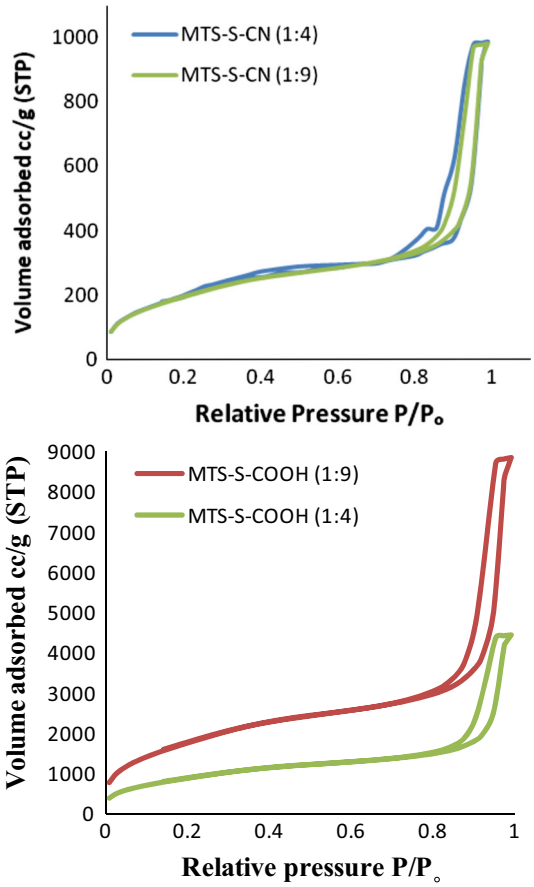

Fig. 3 MTS-S-CN (1:4), MTS-S-CN (1:9), MTS-S-COOH (1:9) and MTS-S-COOH (1:4) nitrogen adsorption isotherms

3.2 Atomic force microscopy (AFM) results

The materials prepared by using sunflower oil as a surfactant have small size grain averaged at (0.12 ± 0.08 μm) compared to (0.25 μm) obtained from cardanol [19] and cashew nut liquid [20]. Such materials with small grain-sized morphology (Fig. 4) and high surface area are good

Table 1 Porosity properties of as prepared nanosorbents

Material	BET surface area (m^2/g)	Average pore diameter (nm)	Total pore volume (cm^3/g)
MTS-S-CN (1:9)	760.5409	3.5299	0.5907
MTS-S-COOH (1:9)	975.9470	4.6968	0.5669
MTS-S-CN (1:4)	734.1441	10.0608	1.5512
MTS-S-COOH (1:4)	740.1138	6.3599	1.0911
MTS-DDA-CN (1:9)	863.8664	4.4048	0.6018
MTS-DDA-COOH (1:9)	1131.1287	4.6968	0.5534
MTS-DDA-CN (1:4)	565.1181	6.6354	0.3820
MTS-DDA-COOH (1:4)	793.3728	4.2615	0.5119

adsorbents due to the presence of many active adsorption sites. Sunflower oil templated silica seems to give smaller grain particles as compared to particle size obtained by using cardanol and cashew nut shell liquid.

3.3 Electron microscopy results

Figure 5 shows the surface morphology of the nanosorbents by both scanning electron microscopy (SEM) and transmission electron microscopy (TEM). The SEM allowed the visualization of the nanosorbent materials at higher magnification. The electron micrograph for SEM represented in Fig. 5a–d shows agglomerated spherical-like particles. They also display some degree of crystalline nature with rough surfaces. The morphology as displayed by SEM electron micrograph corroborate to that depicted by AFM in Fig. 4, further confirming the spherical-like nature of nanoporous materials. The same morphology is ascertained by TEM images Fig. 5e, f which shows spherical nature of the nanosorbents. While SEM images give us the topography of the material highlighting the pore direction, TEM images give grain orientation and at times pore structure in the material. Particle size as calculated from TEM images ranged from 0.48 to 0.84 μm depending on the type of nanosorbents. These figures tally well with the calculated value from SEM for the same nanosorbents. All nanosorbents prepared had similar spherical morphology from both analyses SEM (ESI Fig. S3) and TEM (ESI Fig. S4).

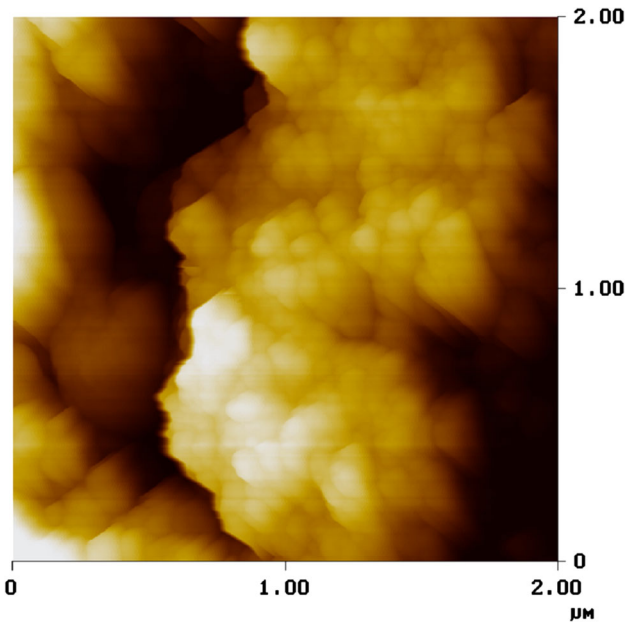

Fig. 4 A three dimensional AFM micrograph for MTS-S-CN

3.4 Diffuse reflectance infrared Fourier transform spectroscopy (DRIFTS)

DRIFTS analysis was used to identify the functional groups in the prepared materials. Results showed that the functional groups were successfully incorporated in all MTS as exemplified by (Fig. 6). The presence of the narrow peak 2350 cm^{-1} (back) and a peak in the range of 1680–1720 cm^{-1} (red), are typical of –CN and –COOH functional group, respectively; after the hydrolysis of MTS-S-CN, the peak at 2350 cm^{-1} disappeared. Furthermore, the presence of a peak at 1740–1800 cm^{-1} indicates the presence of C=O stretching vibration for monomeric carboxylic groups. Thus, incorporation of the –CN group on the material and subsequent hydrolysis, was concluded successful. Similar results have been reported in literature [21]. The downfield shift in the wave number (1680–1720 cm^{-1}) could be due to hydrogen bonding caused by free water molecules present in the MTS-based support by silanols. All prepared nanosorbent materials were analysed to ascertain the presence of desired functional groups (ESI Figs. S5–7).

3.5 Thermal stability of the synthesized materials

The thermal stability of the prepared materials was studied using TGA. Figure 7 indicates weight loss at 53–116 °C for both MTS-S-CN (1:4) and MTS-S-CN (1:9) which may be due to loss of adsorbed water and solvent. This weight loss is followed by other three consecutive weight losses at ±252.6, ±380, and ±583.03 °C which is typical for the decomposition of sunflower oil, normally they correspond to polyunsaturated fatty, monosaturated fatty and saturated fatty [18] which is due to un-removed surfactant (sunflower oil from the nanoporous material The most important part of the TGA results is the stability of the material up 583 °C for MTS-S-CN (1:4) and 568 °C for MTS-S-CN (1:9). It can thus be concluded that the functional groups are chemically bound and hence are thermally stable up to about 600 °C.

3.6 Effect of contact time on the adsorbent

Different time intervals were set to allow the adsorbents to have different contact times with tannery wastewater. The batch adsorptions were therefore carried out at different contact times for an initial chromium (III) ions concentration ranging from 16 to 17.1 mg/L of in the tannery effluent. The percentage removal of chromium (III) at different time intervals were then determined by AAS and the results are graphically presented in (Figs. 8, 9).

The results show that equilibrium time was obtained after 30 min for the initial concentration of Cr(III) ions of

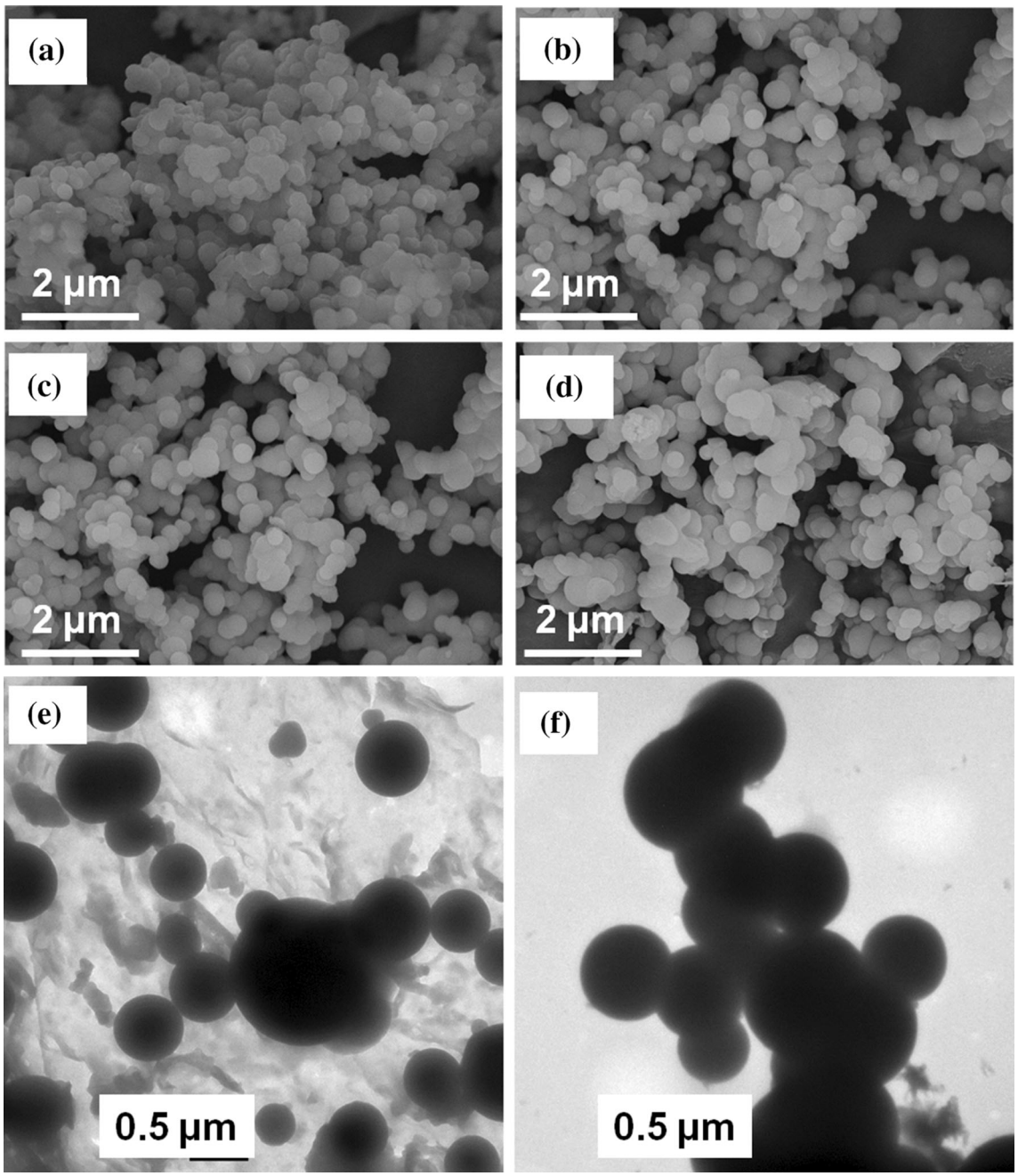

Fig. 5 SEM images of **a** MTS-S-CN (1:4), **b** MTS-S-CN (1:9), **c** MTS-S-COOH (1:4) and **d** MTS-S-COOH (1:9); TEM images of **e** MTS-S-CN (1:4) and **f** MTS-S-COOH (1:9)

16.0–17.1 mg/L. Generally, the removal rate of the adsorbate is rapid initially then slows down later on. The rate of adsorption is higher at the beginning due to monolayer adsorption on the larger surface area of the adsorbent. As the monolayer is saturated, the rate of uptake is controlled by the rate of transport from the exterior to the interior sites of the MTS and hence the rate slows down [21]. The rate of adsorption of MTS-S-COOH was higher as compared to MTS-S-CN. Similarly, the MTS nanosorbents prepared by using *n*-dodecylamine were more efficient than those prepared by using sunflower oil. After 1 h of adsorption, MTS-DDA-COOH 1:9 managed to remove more than 80 % of Cr(III) ions present in the tannery wastewater, while on the other hand, MTS-DDA-CN (1:4) adsorbed only about 60 %. This is in agreement with Hard and Soft Acid Base theory, that hard acids like Cr(III) ions are adsorbed more on hard bases like carboxyl groups than on soft acids such as cyano groups. The same trend was observed for all the prepared materials.

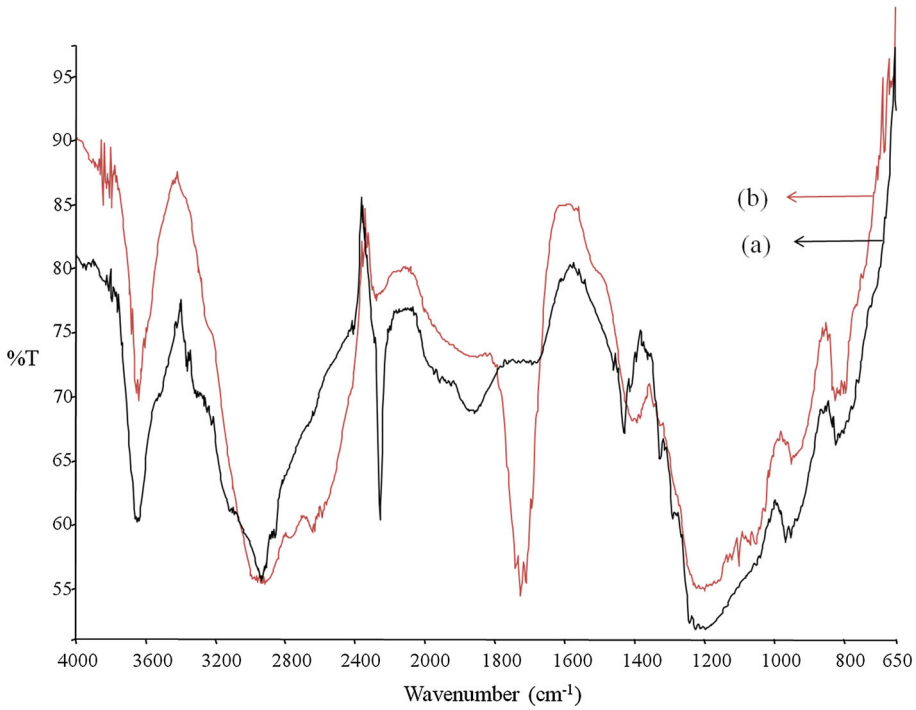

Fig. 6 DRIFT spectra of *a* MTS-S-CN (1:4) and *b* MTS-S-COOH (1:4)

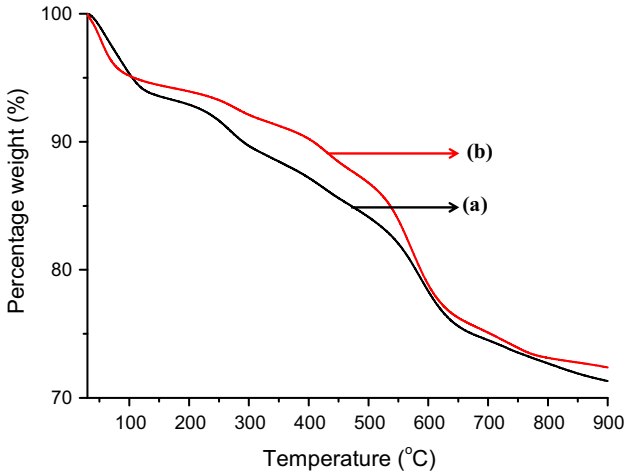

Fig. 7 TGA micrograph for *a* MTS-S-CN (1:4) and *b* MTS-S-CN (1:9)

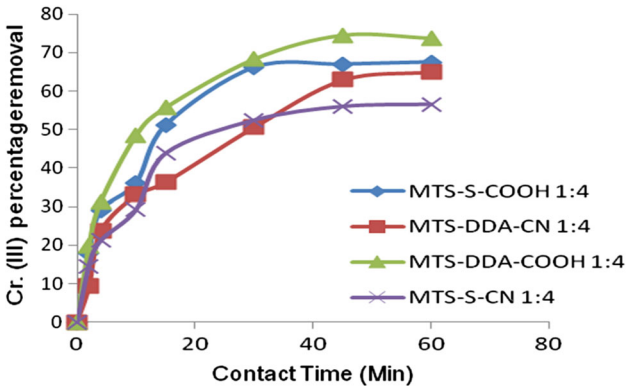

Fig. 8 Effect of contact time on chromium(III) ions removal using MTS (1:4) (initial Cr(III) conc. 17.01 mg/L, pH = 5.2 and 28 °C)

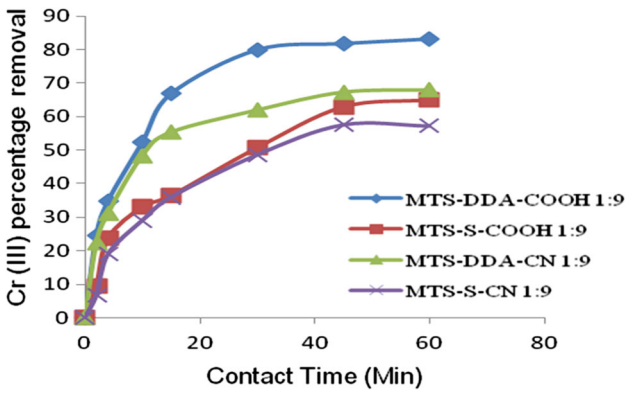

Fig. 9 Effect of contact time on chromium (III) ions removal using MTS (1:9) (initial Cr(III) conc. 17.01 mg/L, pH = 5.2 and 28 °C)

The high efficiency of MTS prepared at the ratio of 1:9 (CETS: TEOS) indicates higher load over 1:4 could be attributed to steric effects, thus providing more active sites for adsorption. This is well supported by BET results where materials prepared at this ratio have higher surface area as compared to those of 1:4 ratios (Table 1).

3.7 Effect of adsorbent amounts

The influence of the adsorbent concentration on the efficiency of Cr(III) removal, is graphically represented in

(Figs. 10, 11). The results indicate that the percentage removal of Cr(III) ions increases as the amount of adsorbent increases up to 0.3 g of the adsorbent; no significant increase is observed above 0.3 g (Fig. 11). This trend is explained by the reality that as you increase the adsorbent, the number of active sites increases, thus a remarkable increase in the uptake of Cr(III) ions. As the maximum adsorption efficiency of Cr(III) is attained, (at 0.3 g of adsorbents) there is no longer a significant increase in the uptake of the metal ions. This result indicates that there is a maximum dosage for each adsorbent; once the maximum amount has been attained [22] the remaining ions in the solution remain constant even if you increase the adsorbent amount.

3.8 Effect of initial Cr(III) ion concentration

The effect of initial chromium(III) ion concentration on the adsorption efficiency or capacity of different adsorbents at a fixed amount (0.2 g) was studied. The experiments were performed at room temperature with contact time of 30 min. The results are provided in (Figs. 12, 13). According to literature reports the chromium(III) uptake is dependent on the initial concentration of the metal in the effluent [22–24]. At low concentrations, the percentage removal was higher due to a larger surface area of the MTS (adsorbent) being available for the adsorption of chromium(III) ions while at higher concentration, the opposite was observed due to limited adsorption sites.

3.9 Mechanism of chromium (III) adsorption by nanosorbents

The superiority of nanosorbents with carboxylic functionality over cyano functionalized nanosorbents in adsorbing Cr(III) can be attributed to the mechanism with which

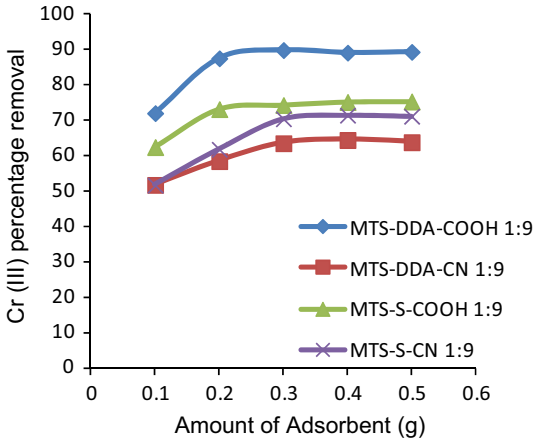

Fig. 10 Effect of different amount MTS (1:9) on chromium(III) ions removal at a conc. of 17.01 mg/L, pH = 5.2 and 28 °C in 30 min

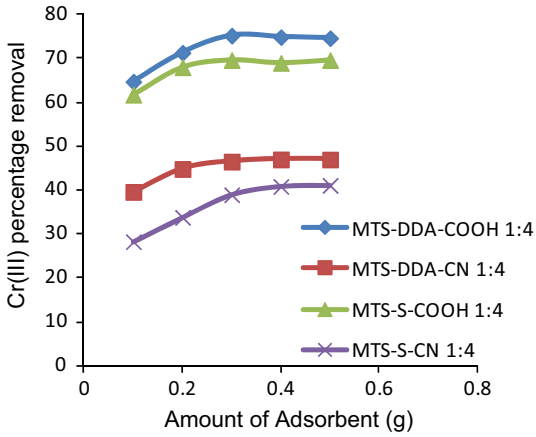

Fig. 11 Effect of different amounts of MTS (1:4) on chromium (III) ions removal at a conc. of 17.01 mg/L, pH = 5.2 and 28 °C in 30 min

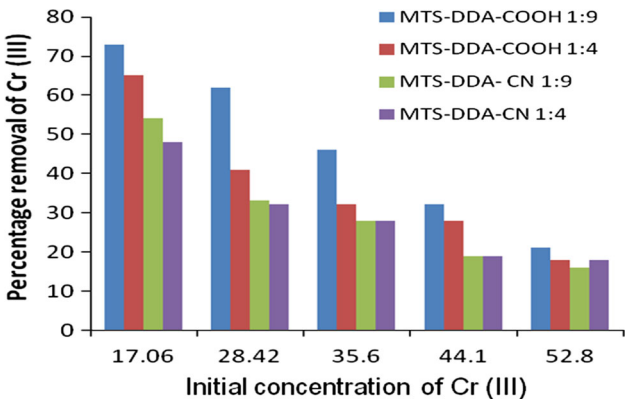

Fig. 12 Effect of initial concentration of Cr(III) ions on different types of MTS prepared using DDA as a template

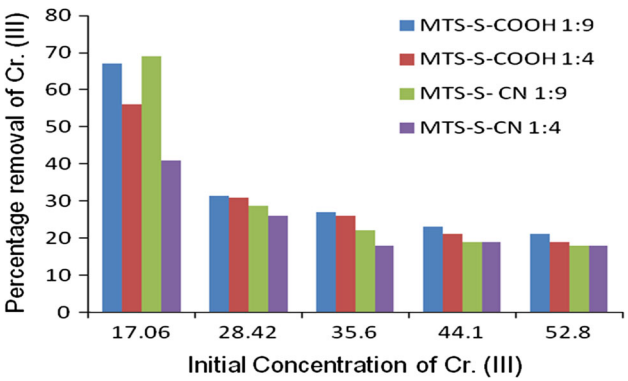

Fig. 13 Effect of initial concentration of chromium(III) ions on different MTS prepared by using Sunflower oil as a template

Cr(III) is adsorbed by nanosorbents. Depending on pH, Cr(III) in aqueous solution exists as soluble Cr^{+3}, and $Cr(OH)^{2+}$, $Cr(OH)_2^+$, $Cr(OH)_3$, or $Cr(OH)_4^-$ ions [11, 25]. In all these compounds, the coordination number of Cr(III) is 6 and this favours carboxylic functionality more than cyano functionality to form complexes of Cr(III). The

mode of binding of Cr(III) to carboxylic groups has previously been studied [26]. The mechanism is further favoured by Pearson's Hard Soft Acid Base Principle (HSAB) where hard acids prefer to bind to *hard* bases and soft acids prefer to bind to *soft* bases. Cr(III), is a hard Lewis acid, and hence would prefer to bind to hard Lewis bases like oxygen-donor ligands rather than cyano group a soft Lewis base in agreement with HSAB theory [27]. The higher surface area for carboxyl-functionalized nanosorbent over cyano-functionalized is not well documented in literature; however it can be attributed to the hydrolysis of cyano-functionalized nanosorbent. The cyano-functionalized nanosorbent is converted into carboxyl-functionalized nanosorbent via hydrolysis which may cause collapse of some pores leading into much smaller total pore volume and hence an increase in the surface area for carboxyl-functionalized nanosorbent.

3.10 Adsorption isotherms

The Langmuir and Freundlich equations were used to simplify and interpret the data derived from the adsorption of Cr(III) ions found in tannery wastewater by nanoporous material over the entire concentration range studied i.e., 5.4 to 62.5 mg/L. The linear plot of Langmuir and Freundlich equations are represented in Figs. 14 and 15 respectively.

Figures 14 and 15 depict the Langmuir and Freundlich isotherms. They describe the data derived from the adsorption of chromium(III) ions from tanneries waste water by MTS-S-COOH over the concentration range of 5.4 – 62.5 mg/L. The linearized forms for both Languimir and Freundlich isotherms [28, 29] indicated that the experimental data for MTS-S-COOH fitted well in both isotherms over the whole range of concentration studied. Important parameters drawn from Langmuir and Freundlich plots i.e. Figs. 14a, b and 15a, b are summarised in Table 2.

The coefficient correlations R^2, for Langmuir isotherm were 0.9517 for MTS-S-COOH (1:9) and 0.9222 for MTS-S-COOH (1:4). The q_m was evaluated and found to be 19.69 mg/g for MTS-S-COOH (1:9) and 13.81 mg/g for MTS-S-COOH (1:4) while K_L for MTS-S-COOH (1:9) was 0.1508 L/mg and 0.220 L/mg for MTS-S-COOH (1:4). The values of separation parameter, R_l was found to be 0.4945–0.0959 for MTS-S-COOH (1:9) while for MTS-S-COOH (1:4) it was found to be 0.4552–0.0817 over a concentration range of 5.4–62.5 mg/L. Since $0 < R_L < 1$, then the Languimir isotherm is favourable [30].

Similarly, the linear plot for Freundlich isotherm indicated that the correlation coefficient, R^2, was found to be 0.9833 for MTS-S-COOH 1:9 and 0.9773 for MTS-S-COOH 1:4. K_f and n values were also determined from the slops of

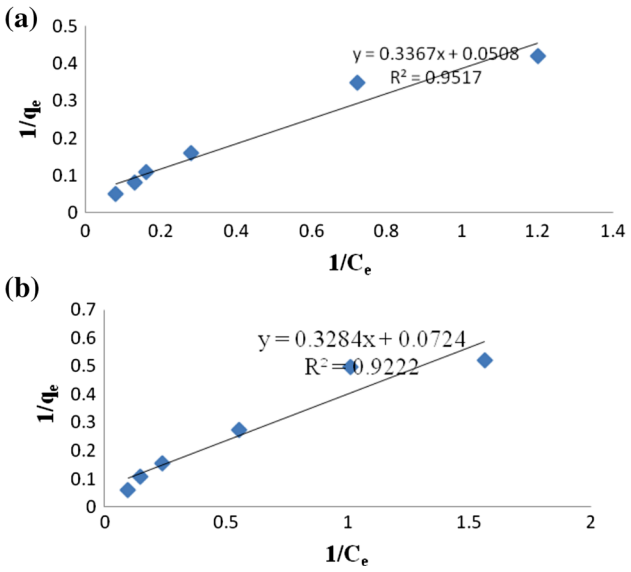

Fig. 14 Languimir adsorption isotherm for chromium (III) ions with **a** MTS-S-COOH 1:9, **b** MTS-S-COOH 1:4

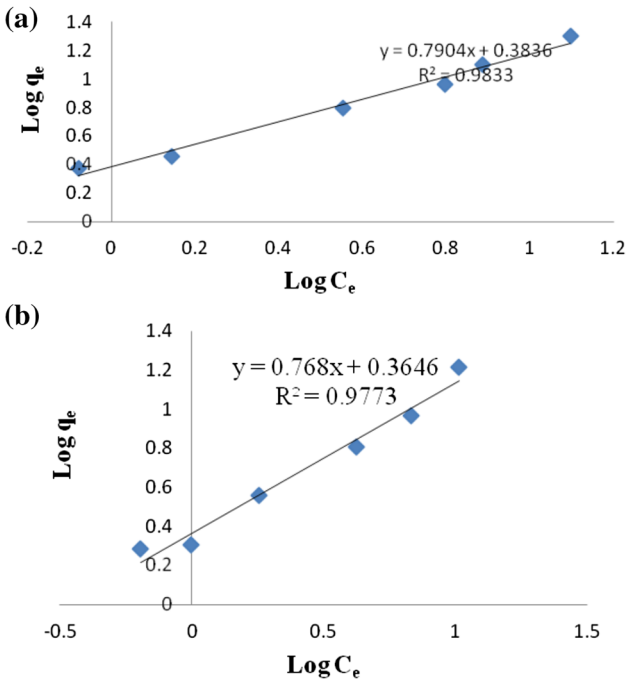

Fig. 15 Linear Freundlich adsorption isotherms for chromium(III) ions with **a** MTS-S-COOH 1:9, **b** MTS-S-COOH 1:4

the Freundlich plots (Fig. 15a, b). MTS-S-COOH 1:9 had $K_f = 2.4188$ and $n = 1.2652$ while MTS-S-COOH 1:4 had $K_f = 2.3153$ and $n = 1.3021$. These values show easy separation of chromium ion from wastewater and high adsorption capacity. The value of n from the two adsorbents was found to be greater than 1, which indicates that adsorption of

Table 2 The values of parameters for each isotherm models used in this study

Isotherm	Adsorbent	Parameter	R^2
Langmuir	MTS-S-COOH (1:9)	$q_m = 19.69$	0.9517
		$K_l = 0.1508$	
	MTS-S-COOH (1:4)	$q_m = 13.89$	0.9222
		$K_L = 0.220$	
Freundlich	MTS-S-COOH (1:9)	$n = 1.2652$	0.9833
		$K_f = 2.4188$	
	MTS-S-COOH (1:4)	$n = 1.3021$	0.9773
		$K_f = 2.3153$	

chromium (III) is favourable, since it is within the beneficial adsorption range of between 1 and 10 [31].

4 Conclusions

This study was investigating the suitability of sunflower oil as a template for the preparation of organically modified MTS. The results have shown that the materials prepared were effective nanosorbents for efficient adsorption of chromium ions from tannery wastewaters. The maximum time for adsorption was established to be 30 min when 0.2 g of the nanosorbent is contacted with tannery wastewater. The adsorption was controlled by parameters such as the amount of the nanosorbent, contact time and initial chromium concentration. Carboxyl-functionalized nanosorbents were better adsorbents than those functionalized with cyano groups due to their high surface area and the nature of Cr(III) ions to bind more easily to carboxylic functionality than cyano functionality. All the prepared materials have proved to be effective nanosorbents at normal conditions, i.e. room temperature and normal pH of tannery wastewater (pH 5.2). It can thus be concluded that the developed technique can serve as an alternative means to obtain nanosorbents suitable for the removal of chromium (III) ions from aqueous solutions, using readily available biodegradable and relatively cheap materials.

Acknowledgments The authors are grateful to the National Research Foundation (NRF) through the South African Research Chair initiative (SARChi) and the NRF (SA)–COSTECH (TZ) Project for financial support.

References

1. S. Kocaoba, Talanta **57**, 23 (2002)
2. I. Gaballah, G. Kilbertus, J. Geochem. Explor. **62**, 241 (1998)
3. J. Romero-González, J.R. Peralta-Videa, E. Rodríguez, M. Delgado, J.L. Gardea-Torresdey, Bioresour. Technol. **97**, 178 (2006)
4. B. Mella, A.C. Glanert, M. Gutterres, Process Saf. Environ. Prot. **95**, 195 (2015)
5. V.J. Sundar, J.R. Rao, C. Muralidharan, J. Clean. Prod. **10**, 69 (2002)
6. M.M. Altaf, F. Masood, A. Malik, Turkish. J. Biol. **32**, 1 (2008)
7. M.E. Argun, Ş. Dursun, J. Int. Environ. Appl. Sci. **1**, 27 (2006)
8. A.A. Belay, J. Environ. Prot. (Irvine, Calif.) **01**, 53 (2010)
9. Stephen Attahirua, Int. J. Phys. Sci. **7**, 1198 (2012)
10. C. Pragathiswaran, S. Sibi, P. Sivanesan, Int. J. Res. Pharm. Chem. **3**, 876 (2013)
11. J. Kotaś, Z. Stasicka, Environ. Pollut. **107**, 263 (2000)
12. S. Avudainayagam, M. Megharaj, G. Owens, R.S. Kookana, D. Chittleborough, R. Naidu, Rev. Environ. Contam. Toxicol. **178**, 53 (2003)
13. S. Tangjuank, N. Insuk, V. Udeye, J. Tontrakoon, Int. J. Phys. Sci. **4**, 412 (2009)
14. C.P. Jordão, J.L. Pereira, G.N. Jham, Sci. Total Environ. **207**, 1 (1997)
15. J.S. Beck, J.C. Vartuli, W.J. Roth, M.E. Leonowicz, C.T. Kresge, K.T. Schmitt, T.W. Chu, D.H. Olson, E.W. Sheppared, S.B. McCullen, J.B. Higgins, J.L. Schlendker, J. Am. Chem. Soc. **114**, 10834 (1992)
16. C.T. Kresge, M.E. Leonowicz, W.J. Roth, J.C. Vartuli, J.S. Beck, Nature **359**, 710 (1992)
17. B. Lefèvre, A. Galarneau, J. Iapichella, C. Petitto, F. Di Renzo, F. Fajula, Chem. Mater. **17**, 601 (2005)
18. A.-M. Putz, S. Cecilia, C. Ianăşi, Z. Dudás, K.N. Székely, J. Plocek, P. Sfârloagă, L. Săcărescu, L. Almásy, J. Porous Mater. **22**, 321 (2014)
19. A. Bibby, L. Mercier, Chem. Mater. **14**, 1591 (2002)
20. A. Hilonga, J.E.G. Mdoe, L.L. Mkayula, Int. J. Biochem. Phys. **17**, 26 (2009)
21. M. Ibrahim, A. Nada, D.E. Kamal, Indian J. Pure Appl. Phys. **43**, 911 (2005)
22. M.S. Nomanbhay, K. Palanisamy, Electron. J. Biotechnol. **8**, 43 (2005)
23. P.M. Pimentel, R.M.P.B. Oliveira, D.M.A. Melo, M.A.F. Melo, A.L.C. Assunção, G. Gonzales, Braz. J. Pet. Gas **5**, 65 (2011)
24. J. Mai, D. Huang, J. Zou, L. Li, Y. Kong, S. Komarneni, J. Porous Mater. **22,** 301 (2014)
25. A.M. Zayed, N. Terry, Plant Soil **249**, 139 (2003)
26. G.A.L. Rodenas, A.M. Iglesias, A.D. Weisz, P.J. Morando, M.A. Blesa, Inorg. Chem. **36**, 6430 (1997)
27. A.J. Cowan, *Inorganic Biochemistry; An Introduction*, 2nd edn. (Wiley VCH, Inc., Columbus, 1997), pp. 7–15
28. A. Sattar, A. Khan, Turk. J. Chem. **36**, 219 (2012)
29. R. Sime, Infohost.Nmt.Edu **7** (2000)
30. A. Mittal, L. Kurup, J. Mittal, J. Hazard. Mater. **146**, 243 (2007)
31. K. Kadirvelu, C. Namasivayam, Environ. Technol. **21**, 1091 (2000)